

## Article

# Tsunami Hazard Zone and Multiple Scenarios of Tsunami Evacuation Route at Jetis Beach, Cilacap Regency, Indonesia

Fx Anjar Tri Laksono <sup>1,2,\*</sup> , Asmoro Widagdo <sup>2</sup>, Maulana Rizki Aditama <sup>2,3</sup>, Muhammad Rifky Fauzan <sup>2</sup> and János Kovács <sup>1</sup> 

<sup>1</sup> Department of Geology and Meteorology, Institute of Geography and Earth Sciences, Faculty of Sciences, University of Pécs, Ifjúság u. 6, 7624 Pécs, Hungary; jones@gamma.ttk.pte.hu

<sup>2</sup> Department of Geological Engineering, Faculty of Engineering, Jenderal Soedirman University, Mayjen Sungkono Rd. KM 5, Purbalingga 53371, Indonesia; asmoro.widagdo@unsoed.ac.id (A.W.); maulana.aditama@postgrad.manchester.ac.uk (M.R.A.); muhammadrifki666@yahoo.co.id (M.R.F.)

<sup>3</sup> Department of Earth and Environmental Sciences, The University of Manchester, Williamson Building, Oxford Road, Manchester M13 9PL, UK

\* Correspondence: anjar93@gamma.ttk.pte.hu

**Abstract:** The 2006 tsunami, throughout the Pangandaran to Cilacap Coast, resulted in 802 deaths and 1623 houses being destroyed. At Jetis beach, Cilacap Regency, 12 people died, and hundreds of houses were damaged. This area is a tourism destination, visited by hundreds of people per week. Therefore, this study aims to determine a tsunami hazard zone and the most effective evacuation route based on multiple factors and scenarios. The method of this study includes scoring, weighting, and overlaying the distance of the Jetis beach from the shoreline and the river, including the elevation and topography. The study results depict five levels of tsunami hazard zone at the Jetis beach: an area of high potential impact, moderately high, moderate, moderately low, and low. The southern Jetis beach is the most vulnerable area with regard to tsunamis, characterized by low elevation, proximity to the beach and rivers, and gentle slopes. The simulation results show the four fastest evacuation routes with the distance from the high-risk zone to the safe zone of around 683–1683 m. This study infers that the southern part of the Jetis beach, in the moderate to high impact zone, needs greater attention as it would suffer worst impact from a tsunami.

**Keywords:** scoring; overlay; evacuation route; tsunami; Jetis; Cilacap; Indonesia



**Citation:** Laksono, F.A.T.; Widagdo, A.; Aditama, M.R.; Fauzan, M.R.; Kovács, J. Tsunami Hazard Zone and Multiple Scenarios of Tsunami Evacuation Route at Jetis Beach, Cilacap Regency, Indonesia. *Sustainability* **2022**, *14*, 2726. <https://doi.org/10.3390/su14052726>

Academic Editors: Stefano Morelli, Veronica Pazzi and Mirko Francioni

Received: 3 February 2022

Accepted: 24 February 2022

Published: 25 February 2022

**Publisher's Note:** MDPI stays neutral with regard to jurisdictional claims in published maps and institutional affiliations.



**Copyright:** © 2022 by the authors. Licensee MDPI, Basel, Switzerland. This article is an open access article distributed under the terms and conditions of the Creative Commons Attribution (CC BY) license (<https://creativecommons.org/licenses/by/4.0/>).

## 1. Introduction

### 1.1. Study Background

In 2006, a tsunami wave with a height of 5–7 m surged along the southern coast of Java. There was a >7 Mw (moment magnitude) earthquake before the tsunami waves hit the southern coast of Java [1,2]. As a consequence of this tragedy, 664 people died, 498 were injured, 1623 houses were damaged, and economic loss reached 55 million US dollars [3]. Earthquakes and tsunamis are the most endangering disaster on the southern coast of Java, because of its location close to the subduction megathrust between the Eurasian continental plate and the Indo-Australian ocean plate [4,5]. Additionally, the Cilacap-Pamanukan-Lematang large fault complex has the potential to induce earthquakes of a magnitude of 7–9 Mw [6,7]. Therefore, there is a need to study tsunami-prone zones throughout southern Java so that people in this area are more alert to avoid vulnerable zones when an earthquake occurs above 7 Mw.

Studies on tsunami wave modeling in southern Java based on 2006 earthquake data have been conducted [8]. This study shows that the height of the tsunami wave in Cilacap was around 3–6 m, and the inundation distance was 400–600 m from the shoreline. Another study on active tectonic deformation in Java using GPS from 2008–2013 found a strain rate of more than one microstrain/year, with an extensional strain of five microstrains/year



## 2. Literature Review

### 2.1. Geo-Tectonic Setting

Jetis beach is situated around 50 km from the shallow earthquake zone and 120 km from the deep megathrust earthquake zone of South Java [27]. The recurrence period for shallow earthquakes ranges from 10–50 years, while the recurrence period for deep earthquakes is not yet known [28]. There is a seismic gap in the medium earthquake zone, where the earthquake's potential magnitude and recurrence period are currently unknown [29]. If we observe the megathrust zone of west Sumatra, the recurrence period for the medium and deep earthquake zones is more extensive than the shallow earthquake zone, and the amount of energy released is more significant and can generate tsunami waves [30,31]. In 2009, an earthquake in Tasikmalaya impacted Jetis Beach, which was 150 km away [32]. This earthquake was generated by the Cilacap-Pamanukan-Lematang active fault zone [33]. Based on USGS data, from 1900 to 2020, there were more than 203 shallow seismic activities with a magnitude of  $\geq 4.5$  Mw [34]. Approximately 80 medium and deep earthquakes occurred in the south of Central Java from 1900 to 2020 with a magnitude greater than 7 Mw [35]. Table 1 summarizes previous studies on the potential for earthquakes and tsunamis in Cilacap.

**Table 1.** Previous studies on the potential for earthquakes and tsunamis in Cilacap. Based on the tectonic setting, Cilacap has a medium earthquake vulnerability, which is dominated by shallow earthquakes. The last earthquake and tsunami in Cilacap occurred in 2006.

Summary	References
Based on the peak ground acceleration at the surface ( $PGA_M$ ) using the probabilistic method, the entirety of Cilacap is classified as having moderate earthquake vulnerability.	[36]
Compilation of fault mechanisms, historical seismograms, calculation of mantle surface waves, and numerical simulations of the tsunami shows that the 1921 earthquake in Cilacap originated from a depth of 30 km. The earthquake mechanism configuration is strike-slip, showing the tensional stress parallel to the direction of convergence with a moment of $5 \times 10^{27}$ dyn cm.	[37,38]
The 2006 earthquake and tsunami in Java had two different rupture stages. The first stage lasted 65 s with a rupture speed of 1.2 km/s. The second stage lasted from 65 to 150 s with a rupture speed of 2.7 km/s.	[39]
There were three primary waves during the 2006 tsunami in West Java–Central Java. The maximum flow depth was up to 5 m, and the maximum run-up height was 15.7 m. Both occurred in Pangandaran, West Java.	[40]

### 2.2. Tsunami Wave and Evacuation Route Simulation

In regards to the study of the potential for earthquakes and tsunamis in Cilacap, research on the tsunami hazard was carried out by [41]. The tsunami hazard probabilistic analysis (PTHA) provides a structured way to integrate multiple sources, including uncertainty due to natural variability and limited knowledge. PTHA-based outcomes are related to average return periods (ARPs). The PTHA composite map provides information on the source of the earthquake, the travel time, and the inundation distance of the tsunami waves on the coast. The earthquake risk map takes into account the integration method of geographic information system (GIS) and field observation data, which have been applied to reduce the risk of earthquakes and tsunamis in Padang and Yogyakarta, Indonesia. The earthquake source in Padang is the Mentawai Islands megathrust. Meanwhile, the trigger of earthquakes and tsunamis in Yogyakarta is the Sunda megathrust along the south of Java. The use of the scoring method in determining the tsunami hazard zone in Padang and Yogyakarta takes into account elevation, slope, and the distance from the coastline [42,43]. The tsunami hazard zone can be determined using a weighting method of

four parameters, namely the distance of a location from the shoreline (Table 2), the distance of the river to the study area (Table 3), slope (Table 4), and elevation. (Table 5). In addition to the weighting method, there are other methods to determine the tsunami hazard zone, including the method developed by [44]. This method is based on calculating the loss of tsunami height per 1 m of inundation distance by including the manning roughness and slope coefficient factors.

**Table 2.** Weights and scores for the distance of a location from the shoreline [45].

No.	Distance (m)	Score	Weight	Total Score
1	<556	1	20	20
2	557–1400	2	20	40
3	1401–2404	3	20	60
4	2405–3528	4	20	80
5	>3528	5	20	100

**Table 3.** Weights and scores for the distance of a location from the river [46].

No.	Distance (m)	Score	Weight	Total Score
1	0–450	1	10	10
2	451–900	2	10	20
3	901–1350	3	10	30
4	1351–1800	4	10	40
5	1801–2250	5	10	50
6	>2250	6	10	60

**Table 4.** Weight, scores, and the type of slope based on the percentage of slope [45].

No.	Percentage of Slope	Type of Slope	Score	Weight	Total Score
1	0–2	Flat	1	10	10
2	2–6	Flat–Gentle	2	10	20
3	6–13	Gentle–Tilt	3	10	30
4	13–20	Tilt	4	10	40
5	20–55	Tilt–Steep	5	10	50
6	>55	Steep–Very Steep	6	10	60

**Table 5.** Weights and scores for the elevation parameter [45,47].

No.	Elevation (m)	Score	Weight	Total Score
1	0–5	1	25	25
2	6–10	2	25	50
3	11–15	3	25	75
4	16–20	4	25	100
5	>20	5	25	125

The method used to create the fastest evacuation route is Dijkstra’s algorithm. This algorithm requires data to be coordinates of each evacuation point, coordinates of each intersection point, and the number of intersections to be passed. Dijkstra’s algorithm can solve the search for the shortest path between two vertices in a weighted graph with the most negligible total weight [48,49]. The concept of the Dijkstra algorithm is to find the shortest distance of a path between two points. The Dijkstra method is not limited to finding the shortest route for tsunami evacuation; it can be applied for other purposes, such as evacuation routes out of buildings during an earthquake or fire [50]. Matlab programming language can function to determine the shortest route for tsunami evacuation using the Dijkstra algorithm. Other parameters besides distance can also be added to determine the best evacuation route: road width, population density, and road conditions. The level of preference determination can adopt the fuzzy logic method [51].

### 3. Materials and Methods

In this study, we used the earthquake and tsunami history in southern Java and the regional geology of Banyumas to determine whether our study area is earthquake and tsunami vulnerable. We collected IFSAR DEM data with a resolution of 5 m, an Indonesian earth map, an Indonesian administrative map, and an Indonesian shoreline map. We used ArcGIS 10.8.1 software to define the boundary of the case study area and the shoreline of Jetis Beach, Cilacap. Spatial data extraction was carried out to obtain a tsunami hazard map based on the specified parameter classification. parameter selection refers to the dominant factors that affect the distribution of tsunami waves on land. In this study, we used four parameters: distance from the shoreline (Table 2), distance from the river (Table 3), slope (Table 4), and elevation (Table 5). Each of these maps has tsunami hazard classes connected to the parameters that have the highest to lowest scores: the distance from the shoreline, elevation, slope, and the distance from the river [52]. Subsequently, we overlay all of them to obtain the final tsunami hazard zone map (Figure 2).



**Figure 2.** Flowchart of tsunami hazard zone mapping at Jetis beach, Cilacap. The final result of this process is determining tsunami hazard map multiple factors.

The tsunami evacuation route at Jetis Beach applies the Dijkstra algorithm using Matlab programming language. The data needed in this case are geographic location, number of inhabitants, transportation path, and evacuation building. We observed the study area to collect them. The starting point and ending point were determined based on the tsunami hazard map at Jetis Beach. The starting point was in the most vulnerable zone of the tsunami, and the endpoint was in the safest zone. The next step was to create a road network that connects the starting and ending points. Clusters and convergence points are represented as a vertex. Meanwhile, road segments are revealed as edges. Then each road network is given a weight based on the fuzzy method by considering the distance traveled, road conditions, population density, and the availability of evacuation buildings. Afterward, we made an m-file using the MATLAB application based on the Dijkstra algorithm. The flow chart of this research can be seen in Figures 3 and A1. The available tsunami evacuation routes were validated built upon actual conditions in the case study area. We conducted field observations to interview residents about whether they were familiar with the available evacuation routes. Community knowledge on evacuation routes will determine the success of the evacuation process [53]. In addition, we also re-checked the road capacity and the availability of evacuation buildings to accommodate the existing population.

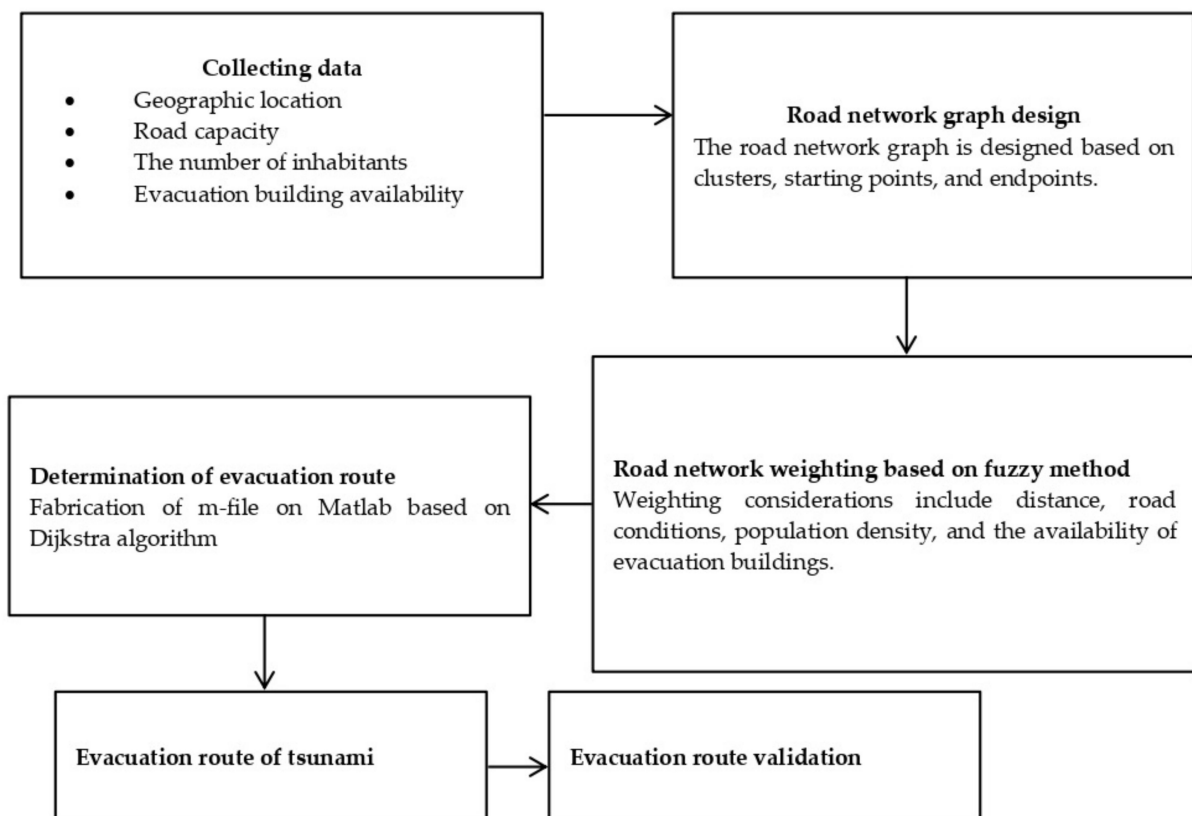


**Figure 3.** Flowchart of establishing tsunami evacuation routes at Jetis Beach using Dijkstra algorithm.

#### 4. Results

The level of tsunami susceptibility is based on four parameters, including elevation, distance from shoreline, slope, and distance from rivers. The farther an area is from the coastline; the less likely a tsunami wave can reach that area. This can be seen in Figure 4, where the Jetis area and its surroundings are divided into four classes. The first class is an area that is less than 1400 m from the coastline, shown in red on the map. The second class is the area that is 1401–2404 m from the coastline, displayed in yellow on the map. The third class is an area that has a distance of 2404–3528 m from the Jetis coastline, described

in light green on the map. The fourth class is the area with a distance of more than 3528 m from the coastline, illustrated in dark green on the map.

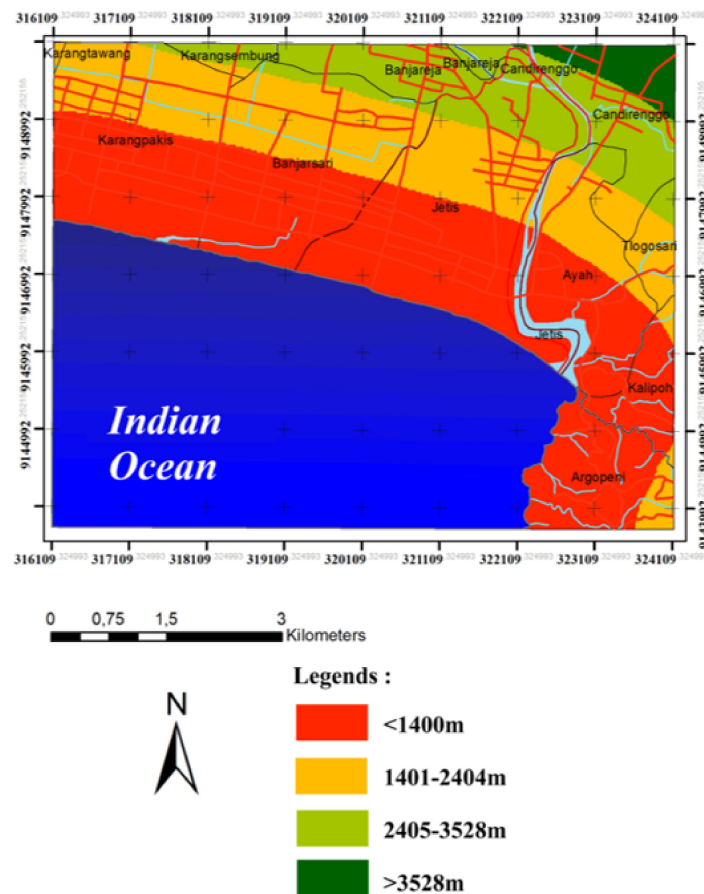


**Figure 4.** The tsunami hazard zone map of Jetis beach based on the distance from the coastline, divided into four classes: less than 1400 m, 1401–2404 m, 2405–3528 m, and more than 3528 m.

The higher the elevation of an area, the lower the possibility that tsunami waves will inundate that area. The elevation map of the Jetis area and its surroundings in Figure 5 consists of four classes. The first class is an area that has an altitude of 0–5 m above sea level, which is depicted in red on the map. The second class is an area that has a height of 5–10 m above sea level, indicated in yellow on the map. The third class is an area that has a height of 10–20 m above sea level, which is exhibited in light green on the map. The fourth class is an area that is at an elevation of more than 20 m, represented in dark green on the map.

In Figure 6, the slopes of the Jetis area and its surroundings are divided into four classes, namely 0–6%, 6–13%, 13–20%, and more than 20%. Based on the correlation analysis between the slope and the level of tsunami hazard, we infer that most of the Jetis area has a slope of 0% to 6%. This indicates that most of the Jetis area and its surroundings have flat slopes. The flat slopes are not adequate to withstand the waves of seawater because there are no barriers used as natural breakwaters to reduce the transportation energy of the tsunami wave. Therefore, the tsunami waves have the potential to flood landward with high transportation energy and strong currents.

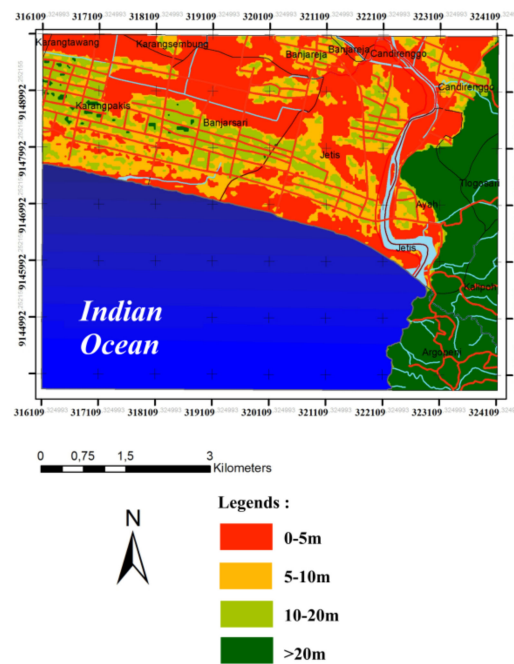


**Figure 5.** Based on elevation, the tsunami hazard zone at Jetis beach consists of four classes: 0–5 m, 5–10 m, 10–20 m, and more than 20 m.

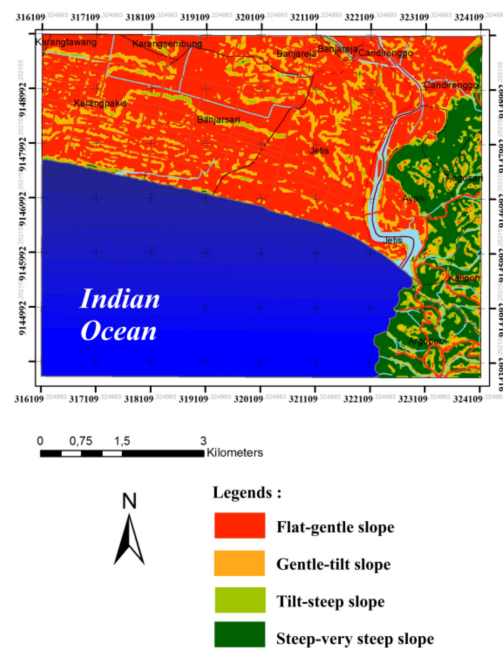


**Figure 6.** Based on the slope, the tsunami hazard zone at Jetis beach is divided into four classes: flat–gentle, gentle–tilt, tilt–steep, and steep–very steep.

Based on Jetis beach’s distance from the river, there are four levels of the tsunami hazard zone, namely less than 900 m, 900–1800 m, 1800–2250 m, and more than 2250 m (Figure 7). Rivers are considered a medium for spreading the inundation of tsunami waves. When the river’s capacity is unable to accommodate the water volume, the area around the river will be inundated. The increasing water discharge will increase the possibility of overflowing around the riverbanks. Therefore, we can assume that the farther an area is from the river, the less likely that area will be flooded by the tsunami waves.

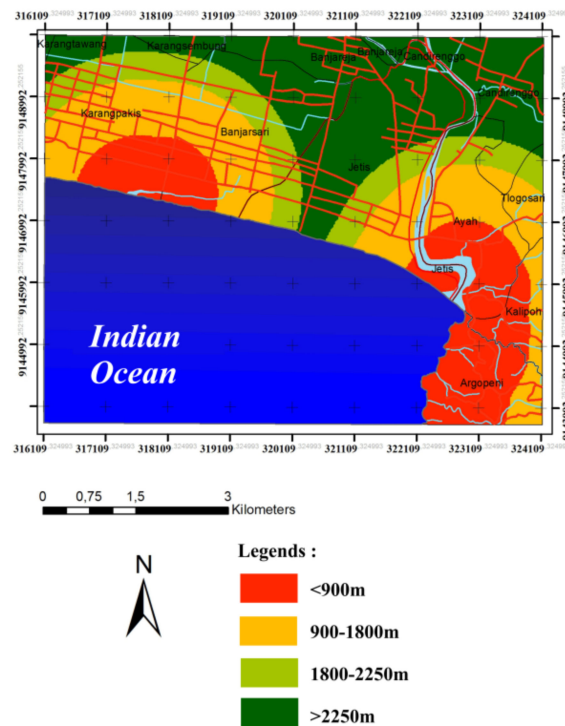


**Figure 7.** Based on the distance of Jetis beach to the river, the tsunami hazard zone is categorized into four levels: less than 900 m, 900–1800 m, 1800–2250 m, and more than 2250 m.

## 5. Discussion

Based on the scoring and weighting of the elevation, Jetis beach's distance to the river and sea, and the topographic map (Figure 8), the tsunami hazard map consists of five zones, ranging from high to low tsunami impact potential zones. The red area has the most significant potential when a tsunami occurs. The orange area has a relatively high potential, and the area with yellow color is classified as medium potential. The light green color represents a low impact of tsunami waves. The darker green colored areas have the lowest impact from tsunami waves.

The tsunami hazard map on Jetis beach comprises five levels. The southernmost area of the beach has a high vulnerability, with typical low elevation, close to the coast and the river, and a relatively gentle slope. Meanwhile, the northern part of Jetis beach has a medium risk from tsunamis, characterized by a medium elevation, far distance from the coastline, close proximity to the river, and medium slopes. The low-risk tsunami hazard zone is in the eastern part of Jetis beach, with high elevations, close proximity to the river, and steep slopes (Figure 8).

Jetis Village, Banjarsari Village, and Karangpakis Village have a high risk of tsunami vulnerability. These areas are adjacent to the coastline and have a low elevation. Purwodadi Village, Karangsembung Village, Klumprit Village, Banjareja Village, Kedungbenda Village, Candirenggo Village, Wangunweni, and Ayah Village are at moderate-risk of tsunami hazards. Their distance is somewhat far to the coastline, and they have a relatively high elevation. Meanwhile, Tlogosari Village, Argopeni Village, and Kalipoh Village have a low risk of tsunami hazard because these villages have a high elevation, a steep slope, and are far from the coast. The high-risk to medium-risk zones need more attention in disaster mitigation efforts to reduce the impact of tsunami waves. The solution to mitigate the worst impact of the tsunami in these areas is undertaking an evacuation route simulation that considers the distance from the starting point to the end point and the public road's capacity compared to the number of people who will be evacuated. Moreover, the familiarization of the evacuation route for inhabitants is necessary. Breakwaters such as sea walls and mangrove planting can be relied on to reduce the energy of tsunami waves.

The classification of the level of tsunami vulnerability in this study supports the theory proposed by [54], which uses coastal shape and slope parameters to determine the tsunami hazard zone in an area. This study has mapped the tsunami hazard zone in more detail due to a large scale and a focus on a narrow area, namely the sub-district level, which has never been studied before. Ref. [43] mapped the tsunami vulnerability zone on the southern coast of Java, in the Special Region of Yogyakarta Province. According to [54], each area has its vulnerability zone due to different topographic conditions, population density, and shoreline shape. This study succeeded in revealing the tsunami vulnerability zone in an area that has so far been uncharted. However, this study lacks total accuracy because the use of reference simulations for the height and inundation distance of the tsunami waves only considers the earthquake in 2006. In fact, according to [2], in the south of Java, many seismic gaps could cause a larger moment magnitude of earthquakes as compared to 2006. The results of this research include a preliminary study that needs to be supported by analysis of paleo-tsunami depositional data and simulations of tsunami waves before 2006.

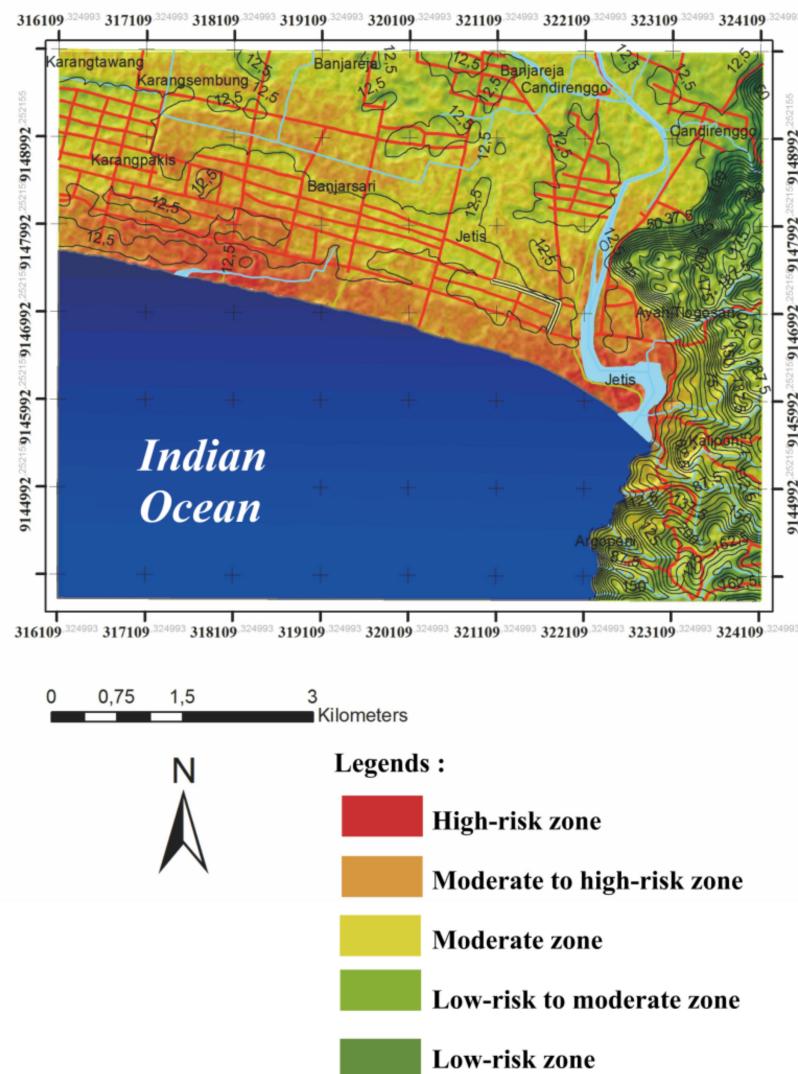


**Figure 8.** Five groups of the tsunami hazard zone based on overlaying Jetis beach's distance from the river and shoreline as well as its elevation and slope: high risk, medium to high risk, medium, medium to low risk, and low risk.

We compared the results of this study with the results of field observations after the 2006 tsunami by [40], which was then supported by simulations of the height and distance of the tsunami wave inundation using COMCOT [8]. The two previous studies stated that

the maximum height of the tsunami waves at Cilacap Beach was only 6 m; this was due to a natural barrier in the form of Nusakambangan Island, so that the height and speed of the tsunami waves were significantly reduced. The inundation distance of the 2006 tsunami was not more than 1 km. The results of interviews with five residents conducted on 19 June 2021 also indicated that the height of the tsunami waves was no higher than a coconut tree, which has a height of about 8–10 m, and the furthest distance from the coastline was no more than 600 m. The five residents are living witnesses of the 2006 tsunami disaster in Cilacap. This comparison indicates that the simulation results using the weighting method are still reliable, especially to describe the distance of the tsunami wave inundation. The high-risk zone in this study is about 1 km, which means it is still accurate and follows the results of field observations by [40] and the 2006 tsunami wave simulation using COMCOT by [8]. However, further studies are needed because the source of the earthquake in Cilacap has not been mapped in detail. It is still possible that there are sources of earthquakes that have the potential to generate tsunamis like the 2004 Aceh tsunami tragedy. The earthquake and tsunami tragedy on Lombok Island and Palu City in 2018 showed that uncharted faults release much greater energy and have high-risk seismicity.

Other methods such as calculation of the tsunami height loss, as developed by [44], can also be used to assess the most appropriate method in describing the tsunami hazard risk in Cilacap. The method developed by [44] uses the Manning roughness coefficient parameter, which affects the height and speed of tsunami waves when they reach the mainland. The higher the Manning roughness coefficient, the lower the height and speed of the tsunami waves. The reduced speed and height of the waves will reduce the propagation of these waves on land. The type of land cover strongly influences the Manning roughness coefficient. For example, an area covered by plantations will have a Manning roughness coefficient greater than that of an open area [44].

Based on the simulation of the fastest route using the MATLAB application, four paths are available to reach the safe point from the emergency point. The four lanes were reviewed by looking at the available road capacity. We considered the condition and the width of the road, because if the road is in bad condition, the community evacuation process will be hampered. The determination of the emergency gathering point considers the maximum capacity to accommodate victims. In the study area, the starting point is at each beach entrance. There are three entrances symbolized as point 1, point 13, and point 16. Meanwhile, the closest emergency gathering point that can accommodate the public and tourists is the At-Taqwa Mosque, symbolized by point 8 and a red triangle, and the Jetis Village football court, which is symbolized by point 19 and the red triangle on the map.

The first route is a route that starts from point 1 to point 8. Based on calculations in the MATLAB application, the fastest route to point 8 from point 1 should go through point 1→4→5→6→7→8, with 1683 m of distance (Figures 9 and A2). The second route is the route from point 1 to point 19. Based on calculations in the MATLAB application, the fastest route to get to point 19 from point 1 must go through point 1→2→23→219, with a distance of approximately 998 m (Figures 10 and A3). The third route is the route from point 13 to point 19. Based on calculations in the MATLAB application, the fastest route to get to point 19 from point 13 must go through point 13→14→15→19, with a distance of approximately 683 m (Figures 11 and A4). The fourth route is the route from point 16 to point 19. Based on calculations in the MATLAB application, the fastest route to get to point 19 from point 16 must go through point 16→17→14→15→19, with a distance of approximately 1125 m (Figures 12 and A5).

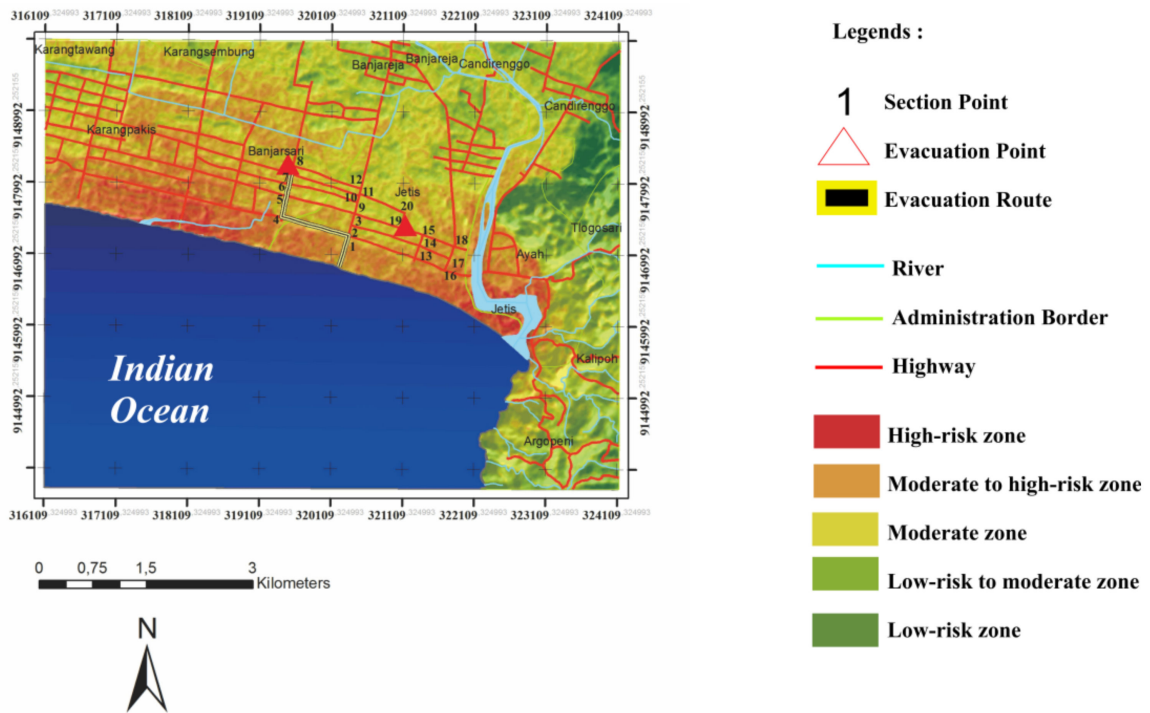


Figure 9. The first evacuation route from point 1, a vulnerable zone, to point 8, a safe zone, is 1683 m.

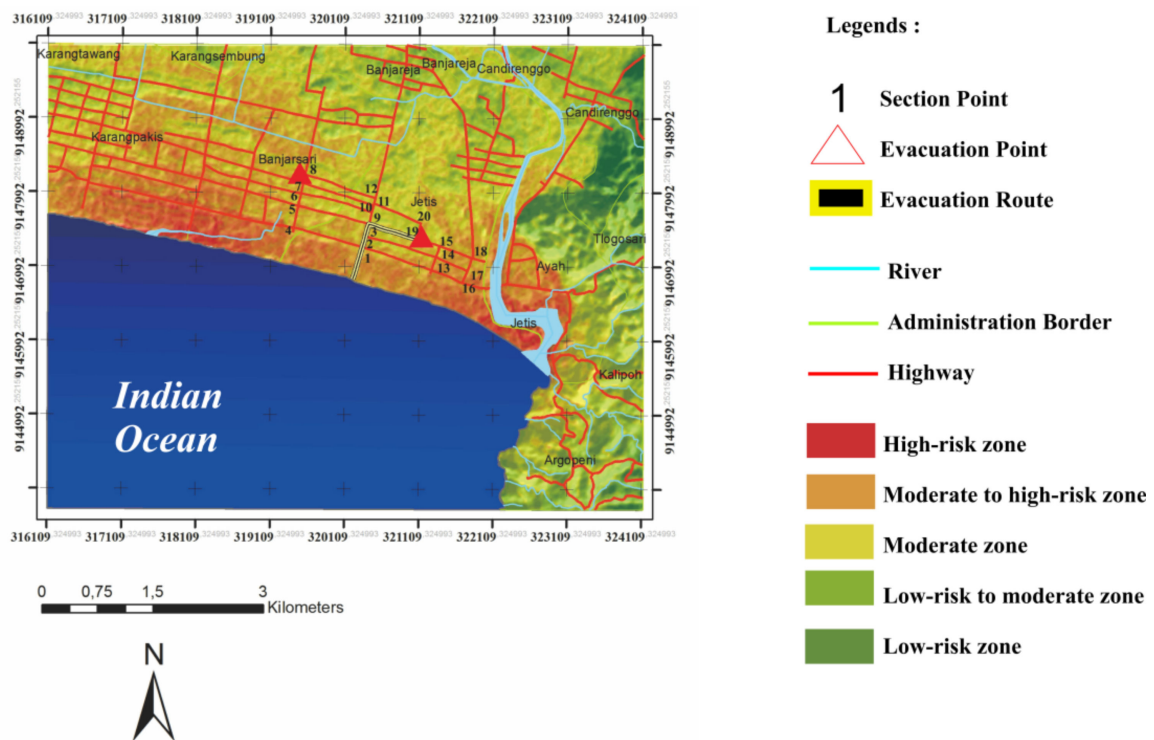


Figure 10. The second evacuation route from point 1, a vulnerable zone, to point 19, a safe zone, is 998 m.

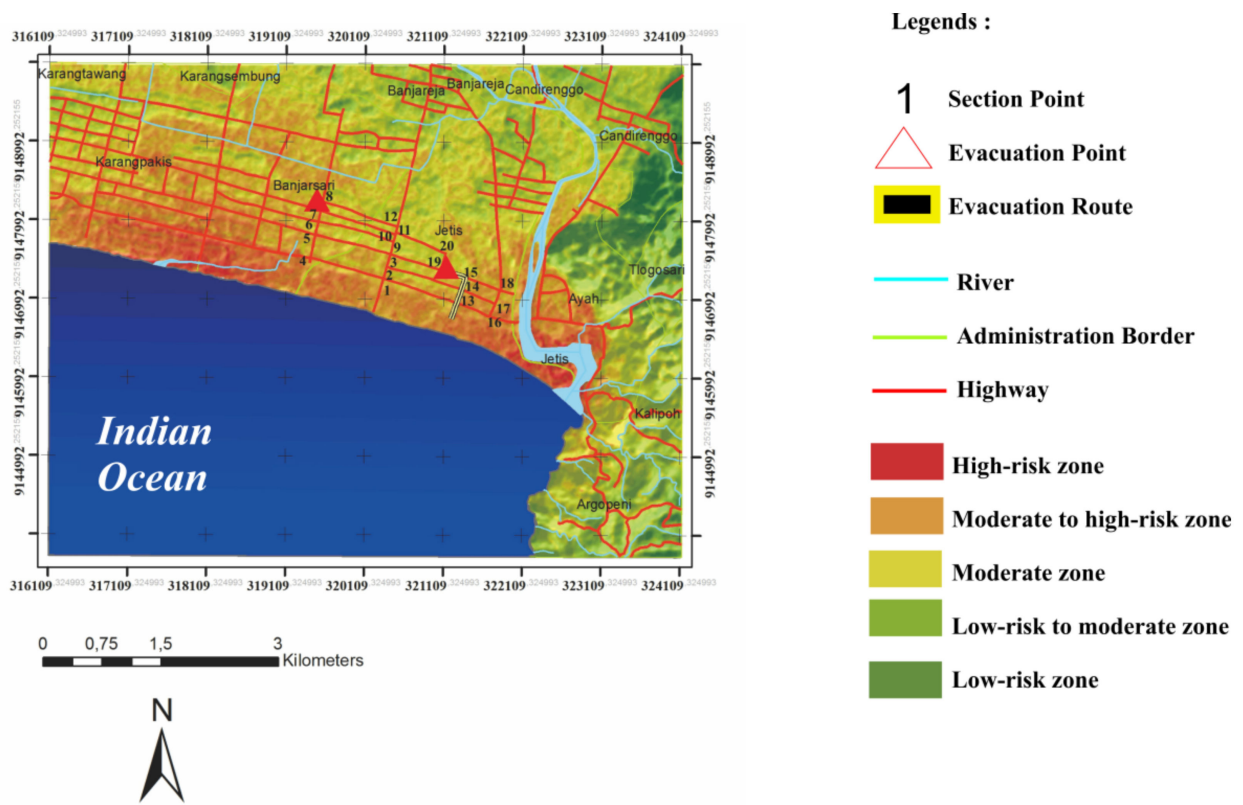


Figure 11. The third evacuation route from point 13, a vulnerable zone, to point 19, a safe zone, is 683 m.

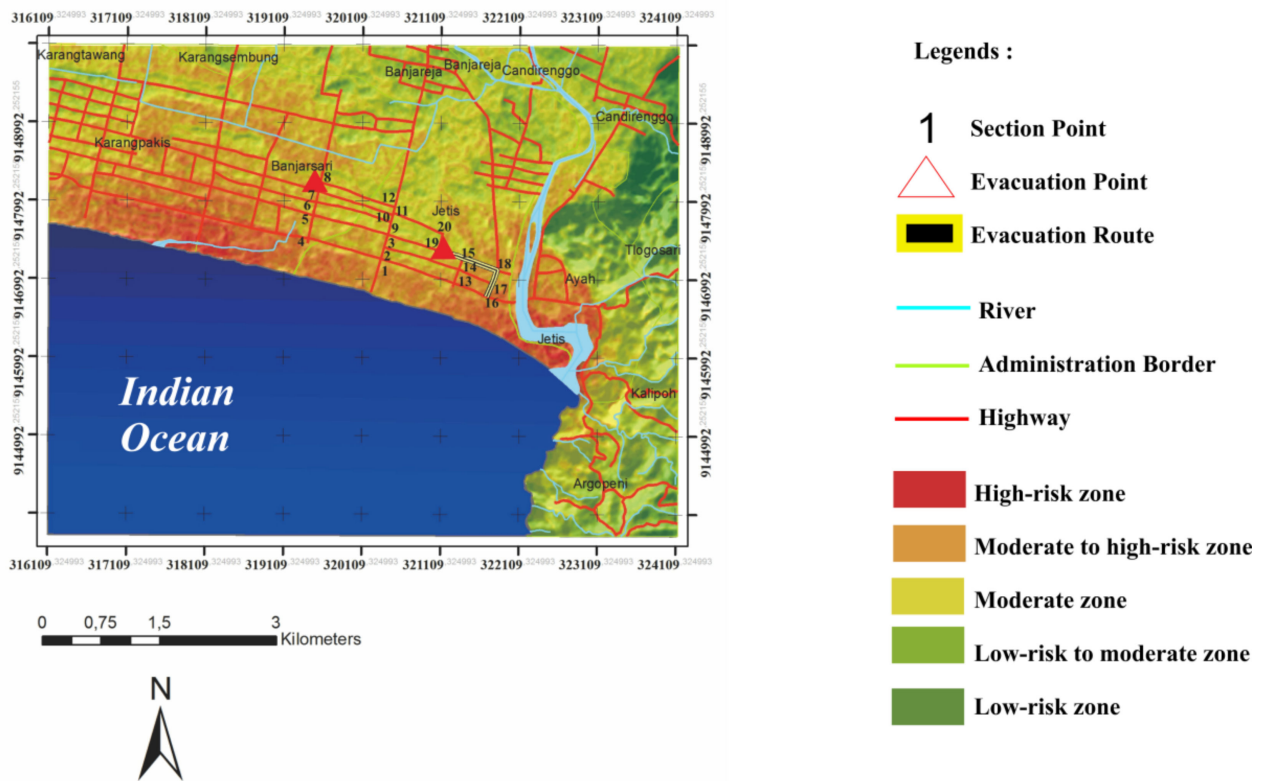


Figure 12. The fourth evacuation route from point 16, a vulnerable zone, to point 19, a safe zone, is 1125 m.

We made observations at the research site to validate the evacuation route that we developed. Evacuation route validation encompasses the distance from the evacuation center location to the temporary shelter, shelter capacity, road capacity, population density, and residents' knowledge of evacuation routes. The validation results show that the four evacuation routes we developed have adequate road capacity and adequate temporary shelters. Residents are also familiar with the evacuation route that we developed because the route passes through the village road, which residents often use to go to work and school. Observations were made on 20 June 2021. In the future, we need to publicize this evacuation route to local society and tourists so that fatalities due to tsunamis tragedy can be minimized.

The results of this study can be used as an initial reference for mapping the tsunami hazard zone along the southern coast of Central Java. Currently, the tsunami hazard mapping in the southern coast of Central Java has not been carried out evenly. Meanwhile, the threat of a tsunami in the future is still considerable. In the south of Java, it is relatively more difficult to predict when a major earthquake will occur compared to the west coast of Sumatra Island. This study also contributed significantly to assisting the government's program to map all tsunami hazard zones in Indonesia, including Java, due to 60% of Indonesia's population living on Java island.

## 6. Conclusions

The weighting and overlaying distance maps from coastlines and rivers, topographic maps, and elevation maps show that the Jetis Beach area and its surroundings consist of five tsunami hazard zones: high-risk zone, moderate to high-risk zone, moderate zone, low to moderate zone, and low-risk zone. The most vulnerable zone is located in the southern part of Jetis beach, while the safest zone lies in the northern and eastern parts of Jetis beach. There are four scenarios of evacuation routes in this case. The distances of each route from the most vulnerable zone in the southern part of Jetis beach to the safest in the north and east of Jetis beach are 683 m, 998 m, 1125 m, and 1683 m. Publicization of tsunami hazard zones and evacuation routes to the community is necessary to minimize casualties and material losses. Furthermore, the construction of sea walls and planting of mangrove trees will help reduce the energy and inundation of tsunami waves when they reach inland.

**Author Contributions:** F.A.T.L. designed the simulations and wrote the article. A.W. analyzed the results of the simulation and reviewed the article. M.R.A. performed the simulations. M.R.F. collected the data. J.K. gave comments and critical notes on the article. All authors have read and agreed to the published version of the manuscript.

**Funding:** This research was funded by National Research, Development and Innovation Office, grant number NKFI K120213 and the APC was funded by the European Union, co-financed by the European Social Fund: EFOP-3.6.1.-16-2016-00004.

**Institutional Review Board Statement:** Not applicable.

**Informed Consent Statement:** Not applicable.

**Data Availability Statement:** The data contained in this study are available in this article.

**Conflicts of Interest:** The authors declare no conflict of interest.

## Appendix A

```

node=xlsread('NODES.xls');
segment=xlsread('SEGMENT.xls');
figure; plot(node(:,2), node(:,3),'b.');
```

ax = gca; % axes handle  
ax.YAxis.Exponent = 0;  
ax.YAxis.TickLabelFormat = '%.0f';  
ax.XAxis.Exponent = 0;  
ax.XAxis.TickLabelFormat = '%.0f';  
hold on;

```

    for s = 1:29
        if (s <= 20) text(node(s,2),node(s,3),[' ' num2str(s)]); end
        plot(node(segment(s,2:3)',2),node(segment(s,2:3)',3),'k');
    end
[d,p]=dijkstra(node,segment,16,19)
for n = 2:length(p)
    plot(node(p(n-1:n),2),node(p(n-1:n),3),'r-','linewidth',2);
end
title(['Shortest Distance from ' num2str(16) ' to ' ...
    num2str(19) ' = ' num2str(d) ' meter '])
hold off;
explanation :
plot=plotting point
xlsread=reads files with .xls format
figure=to display image
node=coordinate at any point
segment=intersection of each intersection
s=sum of segment
num2str=transforms the number into a line
b.=color point to blue
k=color line to black
linewidth=line
r-=color line of distance to red
a=start point
b=point of purpose
title([Shortest Distance From]) = giving a title "shortest distance from"
```

**Figure A1.** The m-file formula of the Dijkstra algorithm was used in the evacuation route map.

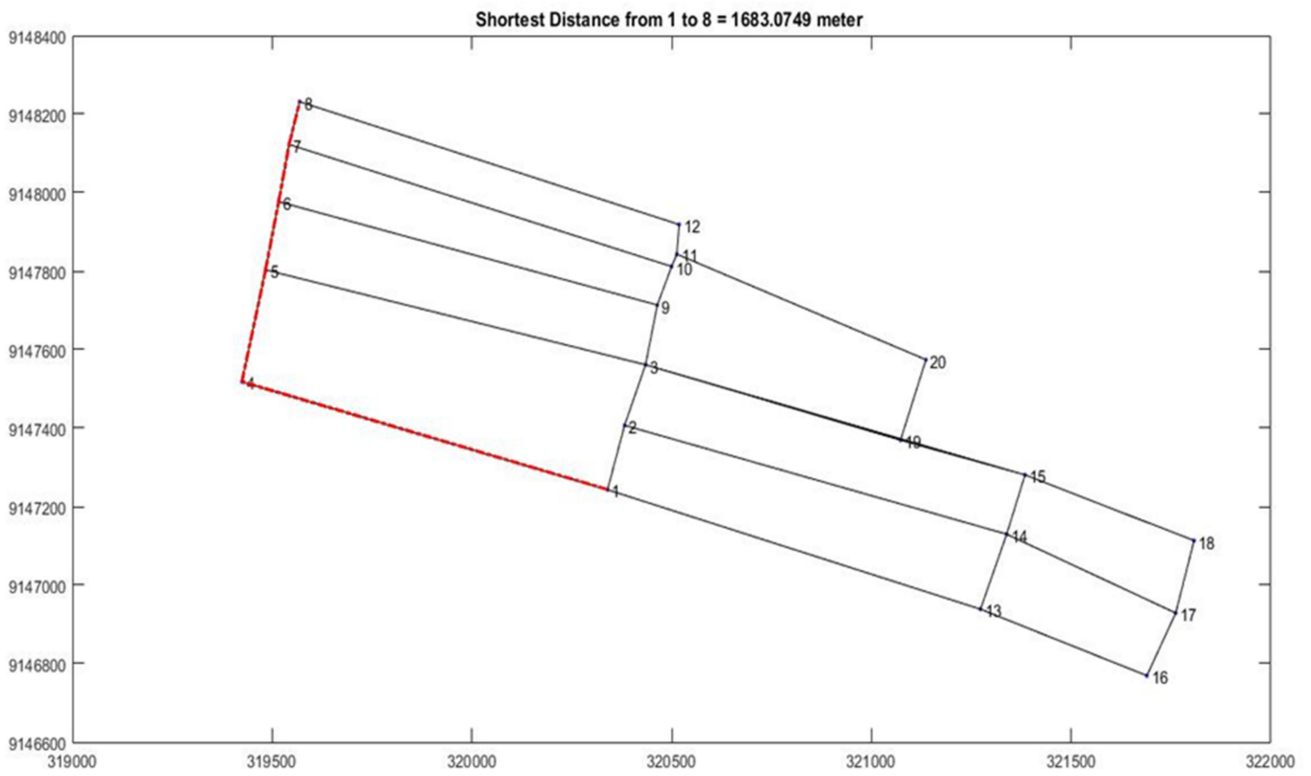


Figure A2. The first evacuation route from points 1 to 8.

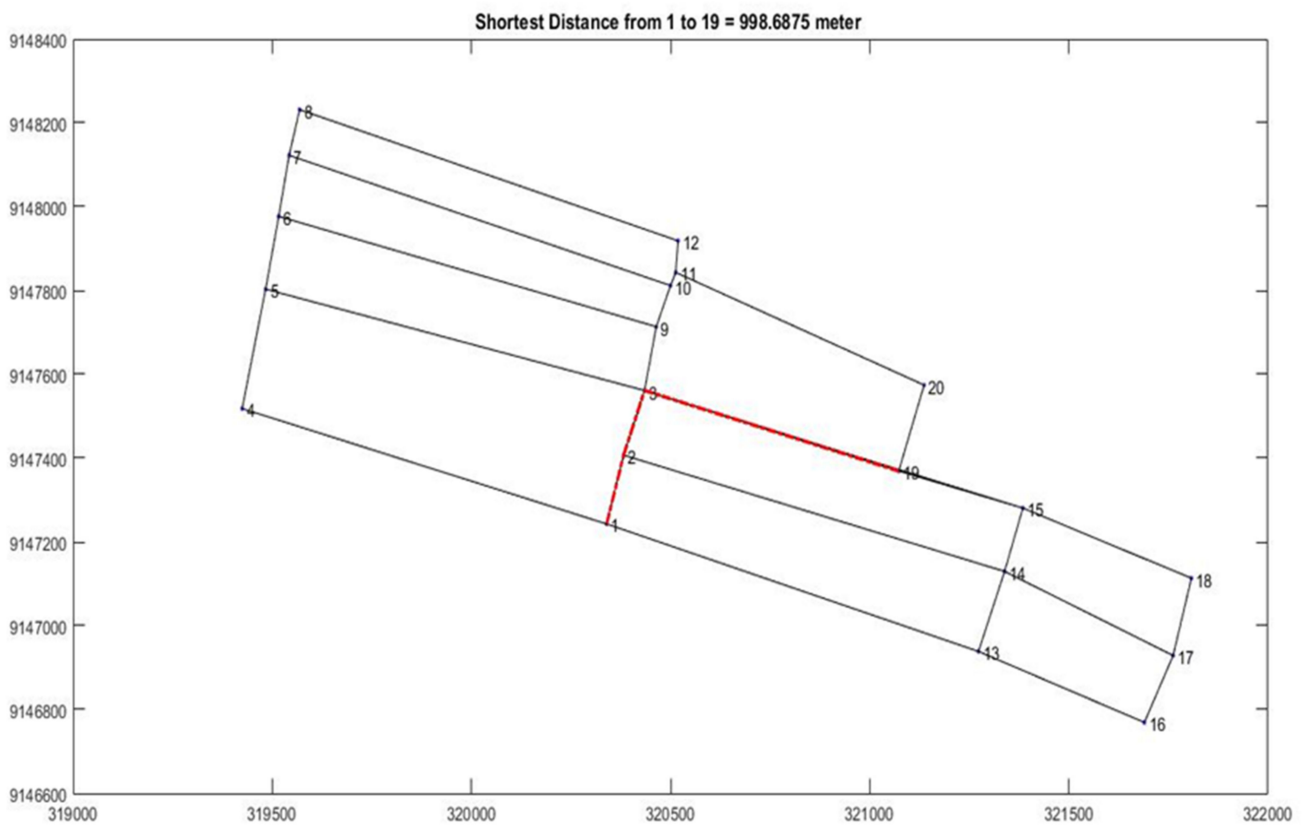


Figure A3. The second evacuation route from points 13 to 19.

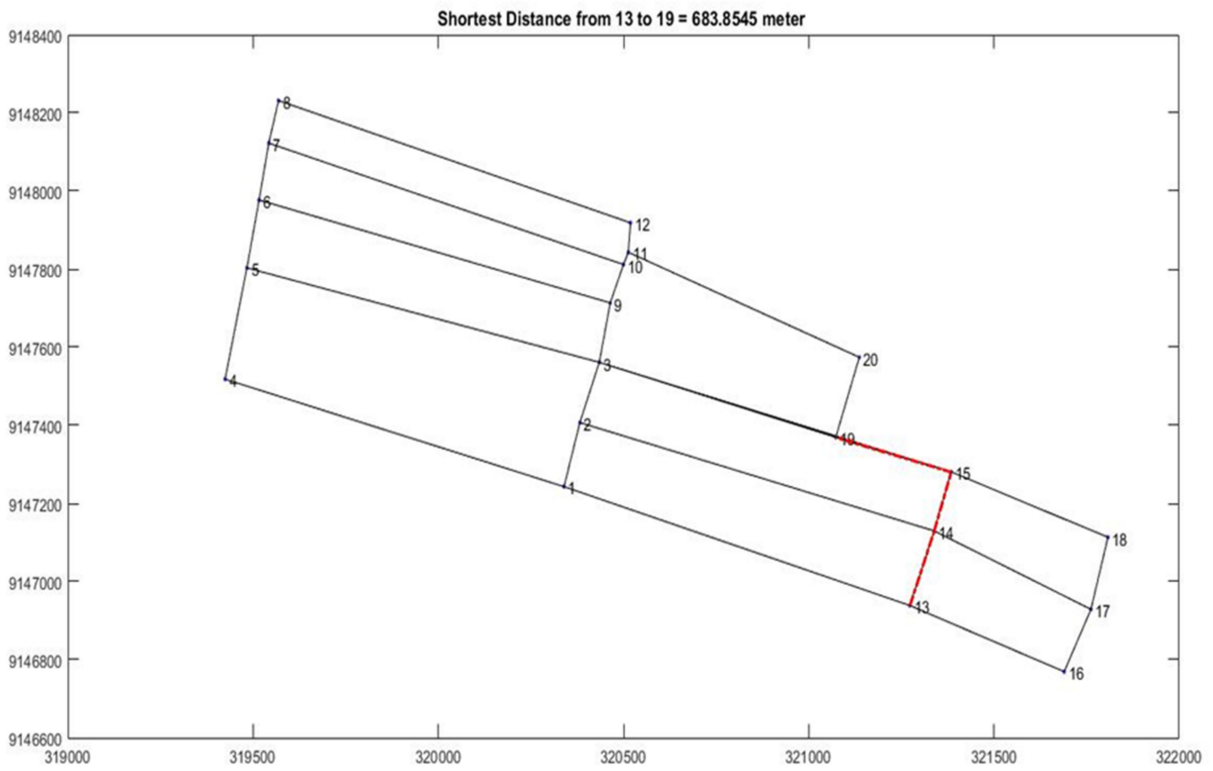


Figure A4. The third evacuation route from points 16 to 19.

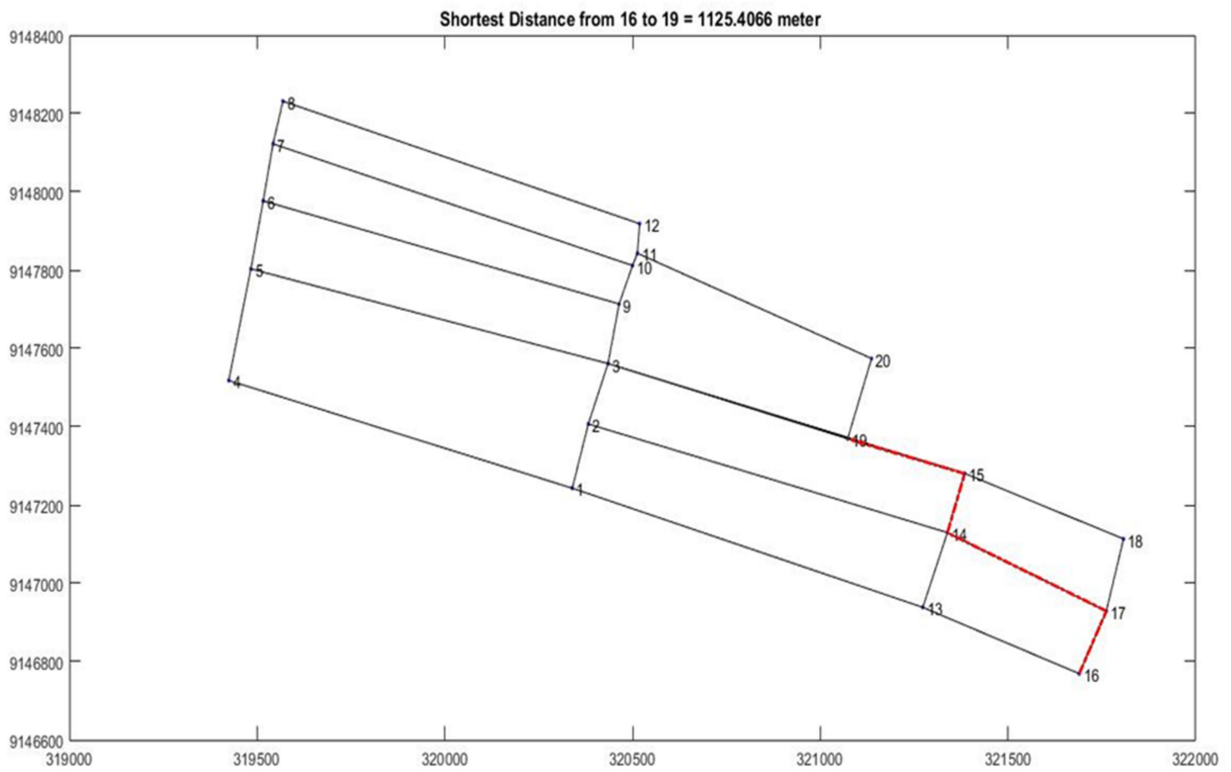


Figure A5. The fourth evacuation route from points 16 to 19.

## References

1. Faiqoh, I.; Gaol, J.L.; Ling, M.M. Vulnerability level map of tsunami disaster in Pangandaran Beach, West Java. *Int. J. Remote Sens. Earth Sci.* **2014**, *10*, 90–103. [[CrossRef](#)]
2. Widiyantoro, S.; Gunawan, E.; Muhari, A.; Rawlinson, N.; Mori, J.; Hanifa, N.R.; Susilo, S.; Supendi, P.; Shiddiqi, H.A.; Nugraha, A.D.; et al. Implications for megathrust earthquakes and tsunamis from seismic gaps south of Java Indonesia. *Sci. Rep.* **2020**, *1*, 15274. [[CrossRef](#)] [[PubMed](#)]
3. BMKG. *Katalog Gempabumi Signifikan Dan Merusak 1821–2017*, 1st ed.; Badan Meteorologi Klimatologi dan Geofisika: Jakarta, Indonesia, 2018; pp. 1–252.
4. Usman, F.; Murakami, K.; Hariyani, S.; Kurniawan, E.B.; Shoimah, F. Tsunami disaster mitigation analysis on the shore of Java Island using CADMAS/Surf numerical simulations. *Disaster Adv.* **2019**, *12*, 1–5.
5. Windupranata, W.; Hanifa, N.R.; Nusantara, C.A.D.S.; Aristawati, G.; Arifianto, M.R. Analysis of tsunami hazard in the Southern Coast of West Java Province-Indonesia. *IOP Conf. Ser. Earth Environ. Sci.* **2020**, *618*, 012026. [[CrossRef](#)]
6. Kato, T.; Ito, T.; Abidin, H.Z.; Agustan. Preliminary report on crustal deformation surveys and tsunami measurements caused by the July 17, 2006 South off Java Island earthquake and tsunami, Indonesia. *Earth Planets Space* **2007**, *59*, 1055–1059. [[CrossRef](#)]
7. Salmanidou, D.M.; Ehara, A.; Himaz, R.; Heidarzadeh, M.; Guillas, S. Impact of future tsunamis from the Java trench on household welfare: Merging geophysics and economics through catastrophe modelling. *Int. J. Disaster Risk Reduct.* **2021**, *61*, 102291. [[CrossRef](#)]
8. Laksono, F.A.T.; Aditama, M.R.; Setijadi, R.; Ramadhan, G. Run-up height and flow depth simulation of the 2006 South Java tsunami using COMCOT on Widarapayung Beach. *IOP Conf. Ser. Mater. Sci. Eng.* **2020**, *982*, 012047. [[CrossRef](#)]
9. Gunawan, E.; Widiyantoro, S. Active tectonic deformation in Java, Indonesia inferred from a GPS-derived strain rate. *J. Geodyn.* **2019**, *123*, 49–54. [[CrossRef](#)]
10. Pribadi, K.S.; Abduh, M.; Wirahadikusumah, R.D.; Hanifa, N.R.; Irsyam, M.; Kusumaningrum, P.; Puri, E. Learning from past earthquake disasters: The need for knowledge management system to enhance infrastructure resilience in Indonesia. *Int. J. Disaster Risk Reduct.* **2021**, *64*, 102424. [[CrossRef](#)]
11. Asri, A.K.; Elya, H.; Duantari, N.; Suryaningsih, E.; Victoria, L.D.D.D. Dual Mitigation System: Database System Combination of EWS and APRS for Disaster Management (Case Study: Malang Southern Coast). *Procedia-Soc. Behav. Sci.* **2016**, *227*, 435–441. [[CrossRef](#)]
12. Nusantara, D.S.C.A.; Windupranata, W.; Hayatiningsih, I.; Hanifa, N.R. Mapping of IOC-UNESCO tsunami ready indicators in the Pangandaran Village, Indonesia. *IOP Conf. Ser. Earth Environ. Sci.* **2021**, *925*, 012041. [[CrossRef](#)]
13. Tappin, D.R. Submarine landslides and their tsunami hazard. *Annu. Rev. Earth. Planet Sci.* **2021**, *49*, 551–578. [[CrossRef](#)]
14. Siagian, T.H.; Purhadi, P.; Suhartono, S.; Ritonga, H. Social vulnerability to natural hazards in Indonesia: Driving factors and policy implications. *Nat. Hazards* **2014**, *70*, 1603–1617. [[CrossRef](#)]
15. Adriano, B.; Xia, J.; Baier, G.; Yokoya, N.; Koshimura, S. Multi-source data fusion based on ensemble learning for rapid building damage mapping during the 2018 Sulawesi earthquake and Tsunami in Palu, Indonesia. *Remote Sens.* **2019**, *11*, 886. [[CrossRef](#)]
16. Dewatama, E. Tsunami hazard mapping and loss estimation in Yogyakarta International Airport Area. *Built Environ. Stud.* **2021**, *2*, 1–11. [[CrossRef](#)]
17. Khomarudin, M.R.; Günter, S.; Ralf, L.; Kai, Z.; Joachim, P.; Widjo, K.; Widodo, P.S. Hazard analysis and estimation of people exposure as contribution to tsunami risk assessment in the west coast of sumatra, the south coast of Java and Bali. *Z. Fur Geomorphol.* **2010**, *54*, 337–356. [[CrossRef](#)]
18. Anwar, K.; Muskananfolo, M.R.; Helmi, M. Spatial analysis of tsunami threat level in the coastal of Jember Regency, East Java, Indonesia. *Asian J. Microbiol. Biotechnol. Environ. Sci.* **2018**, *20*, 1153–1162.
19. Suppasri, A.; Muhari, A.; Syamsidik; Yunus, R.; Pakoksung, K.; Imamura, F.; Koshimura, S.; Paulik, R. Vulnerability characteristics of tsunamis in Indonesia: Analysis of the global centre for disaster statistics database. *J. Disaster Res.* **2018**, *13*, 1039–1048. [[CrossRef](#)]
20. Cahyaning, S.I.; Fadly, U.; Keisuke, M.; Suluh, W.I.N. Geographic information system and weighting technique for tsunami risk assessment in coastal villages of Jember Regency, Indonesia. *Disaster Adv.* **2021**, *14*, 38–50.
21. Horspool, N.; Pranantyo, I.; Griffin, J.; Latief, H.; Natawidjaja, D.H.; Kongko, W.; Cipta, A.; Bustaman, B.; Anugrah, S.D.; Thio, H.K. A probabilistic tsunami hazard assessment for Indonesia. *Nat. Hazards Earth Syst. Sci.* **2014**, *14*, 3105–3122. [[CrossRef](#)]
22. Hall, S.; Pettersson, J.; Meservy, W.; Harris, R.; Agustinawati, D.; Olson, J.; McFarlane, A. Awareness of tsunami natural warning signs and intended evacuation behaviors in Java, Indonesia. *Nat. Hazards* **2017**, *89*, 473–496. [[CrossRef](#)]
23. BPS Cilacap. *Kabupaten Cilacap Dalam Angka 2017*, 1st ed.; Badan Pusat Statistik Kabupaten Cilacap: Cilacap, Indonesia, 2018; pp. 1–299.
24. Siregar, A.S.; Romdoni, T.A.; Prayogo, N.A. Water quality monitoring using WQI method in Cemara Sewu shrimp farm Jetis Cilacap Regency. *IOP Conf. Ser. Earth Environ. Sci.* **2019**, *255*, 012038. [[CrossRef](#)]
25. Lestiani, D.D.; Santoso, M.; Kurniawati, S.; Adventini, N.; Prakoso, D.A.D. Characteristics of feed coal and particulate matter in the vicinity of coal-fired power plant in Cilacap, Central Java, Indonesia. *Procedia Chem.* **2015**, *16*, 216–221. [[CrossRef](#)]
26. Kasikoen, K.M. Urbanization and change in Cilacap Regency. *Procedia-Soc. Behav. Sci.* **2016**, *227*, 70–74. [[CrossRef](#)]
27. Yudhicara, Y.; Zaim, Y.; Rizal, Y.; Aswan, A.; Triyono, R.; Setiyono, U.; Hartanto, D. Characteristics of paleotsunami sediments, a case study in Cilacap and Pangandaran coastal areas, Jawa, Indonesia. *Indones. J. Geosci.* **2013**, *8*, 163–175. [[CrossRef](#)]
28. Gunawan, E.; Meilano, I.; Abidin, H.Z.; Hanifa, N.R.; Susilo. Analysis of coseismic fault slip models of the 2012 Indian ocean earthquake: Importance of GPS data for crustal deformation studies. *Acta Geophys.* **2016**, *117*, 64–72. [[CrossRef](#)]

29. Koulali, A.; McClusky, S.; Susilo, S.; Leonard, Y.; Cummins, P.; Tregoning, P.; Meilano, I.; Efendi, J.; Wijanarto, A.B. The kinematics of crustal deformation in Java from GPS observations: Implications for fault slip partitioning. *Earth Planet. Sci. Lett.* **2017**, *458*, 69–79. [[CrossRef](#)]
30. Rosalia, S.; Widiyantoro, S.; Nugraha, A.D.; Supendi, P. Double-difference tomography of p-and s-wave velocity structure beneath the western part of Java, Indonesia. *Earthq. Sci.* **2019**, *32*, 12–25. [[CrossRef](#)]
31. Silpa, K.; Earnest, A. A note on stress rotations due to the 2004 Mw 9.2 Sumatra-Andaman megathrust earthquake. *J. Earth Syst. Sci.* **2020**, *129*, 187. [[CrossRef](#)]
32. Supendi, P.; Nugraha, A.D.; Puspito, N.T.; Widiyantoro, S.; Daryono, D. Identification of active faults in West Java, Indonesia, based on earthquake hypocenter determination, relocation, and focal mechanism analysis. *Geosci. Lett.* **2018**, *5*, 31. [[CrossRef](#)]
33. Daryono, M.R.; Natawidjaja, D.H.; Sapiie, B.; Cummins, P. Earthquake geology of the Lembang Fault, West Java, Indonesia. *Tectonophysics* **2019**, *751*, 180–191. [[CrossRef](#)]
34. USGS. *20 Largest Earthquakes in the World*, 1st ed.; United States Geological Survey: Reston, VA, USA, 2020; pp. 1–15.
35. Pasari, S.; Simanjuntak, A.V.H.; Mehta, A.; Neha; Sharma, Y. The current state of earthquake potential on Java Island, Indonesia. *Pure Appl. Geophys.* **2021**, *178*, 2789–2806. [[CrossRef](#)]
36. Sutrisna, M.; Sulaeman, C.; Ardi, N.D. Microtremor Methode for Microzonation in Cilacap City. *J. Online Fis.* **2015**, *3*, 2.
37. Aditama, M.R.; Sunan, H.L.; Laksono, F.A.T.; Ramadhan, G.; Iswahyudi, S.; Fadlin. Integrated subsurface analysis of thickness and density for liquefaction hazard: Case study of south Cilacap region, Indonesia. *J. Geosci. Eng. Environ. Technol.* **2021**, *6*, 58–66. [[CrossRef](#)]
38. Okal, E.A. The south of Java earthquake of 1921 September 11: A negative search for a large interplate thrust event at the Java trench. *Geophys. J. Int.* **2012**, *190*, 1657–1672. [[CrossRef](#)]
39. Fan, W.; Bassett, D.; Jiang, J.; Shearer, P.M.; Ji, C. Rupture evolution of the 2006 Java tsunami earthquake and the possible role of splay faults. *Tectonophysics* **2017**, *721*, 143–150. [[CrossRef](#)]
40. Lavigne, F.; Gomez, C.; Giffo, M.; Wassmer, P.; Hoebreck, C.; Mardiatno, D.; Priyono, J.; Paris, R. Field observations of the 17 July 2006 tsunami in Java. *Nat. Hazards Earth Syst. Sci.* **2007**, *7*, 177–183. [[CrossRef](#)]
41. Ashadi, A.L.; Kaka, S.L.I. Ground-motion relations for subduction-zone earthquakes in Java Island, Indonesia. *Arab. J. Sci. Eng.* **2019**, *44*, 449–465. [[CrossRef](#)]
42. Ai, F.; Comfort, L.K.; Dong, Y.; Znati, T. A dynamic decision support system based on geographical information and mobile social networks: A model for tsunami risk mitigation in Padang, Indonesia. *Saf. Sci.* **2016**, *90*, 62–74. [[CrossRef](#)]
43. Steinritz, V.; Pena-Castellnou, S.; Marliyani, G.I.; Reichert, K. GIS-based study of tsunami risk in the Special Region of Yogyakarta (Central Java, Indonesia). *IOP Conf. Ser. Earth Environ. Sci.* **2021**, *851*, 012007. [[CrossRef](#)]
44. Berryman, K. Review of tsunami hazard and risk in New Zealand. *Inst. Geol. Nucl. Sci.* **2006**, *139*, 19–26.
45. Subardjo, P.; Ario, R. Uji kerawanan terhadap tsunami dengan Sistem Informasi Geografis (SIG) di pesisir Kecamatan Kretek, Kabupaten Bantul, Yogyakarta. *J. Kelaut. Trop.* **2016**, *18*, 82–97. [[CrossRef](#)]
46. Khasanah, L.U.; Suwarsito; Sarjanti, E. Tingkat kerawanan bencana tsunami kawasan pantai selatan Kabupaten Cilacap. *Geo Edukasi* **2014**, *3*, 77–82.
47. Shuto, N. Tsunami hazard mitigation. *Proc. Jpn. Acad. Ser. B Phys. Biol. Sci.* **2019**, *95*, 151–164. [[CrossRef](#)] [[PubMed](#)]
48. Darmi, Y.; Soerowirdjo, B.; Wibowo, E.; Ernastuti. Dijkstra algorithm application to determine the evacuation routes simulation earthquake and tsunami in the City Bengkulu based on GIS. *J. Adv. Res. Dyn. Control Syst.* **2019**, *11*, 1871–1887.
49. Triatmadja, R. Numerical simulations of an evacuation from a tsunami at Parangtritis beach in Indonesia. *Sci. Tsunami Hazards.* **2015**, *34*, 50–66.
50. Mirahadi, F.; McCabe, B.Y. EvacuSafe: A real-time model for building evacuation based on Dijkstra’s algorithm. *J. Build. Eng.* **2021**, *34*, 101687. [[CrossRef](#)]
51. Lin, Q.; Song, H.; Gui, X.; Wang, X.; Su, S. A shortest path routing algorithm for unmanned aerial systems based on grid position. *J. Netw. Comput. Appl.* **2018**, *103*, 215–224. [[CrossRef](#)]
52. Titov, V.; Kânoğlu, U.; Synolakis, C. Development of MOST for real-time tsunami forecasting. *J. Waterw. Port Coastal Ocean Eng.* **2016**, *142*, 03116004. [[CrossRef](#)]
53. Kubisch, S.; Guth, J.; Keller, S.; Bull, M.T.; Keller, L.; Braun, A.C. The contribution of tsunami evacuation analysis to evacuation planning in Chile: Applying a multi-perspective research design. *Int. J. Disaster Risk Reduct.* **2020**, *45*, 1–14. [[CrossRef](#)]
54. Mardiatno, D.; Malawani, M.N.; Annisa, D.N.; Wacano, D. Review on tsunami risk reduction in Indonesia based on coastal and settlement typology. *Indones. J. Geogr.* **2017**, *49*, 186–194. [[CrossRef](#)]